Bose-Einstein condensation of strongly correlated electrons and phonons in cuprate superconductors

A. S. Alexandrov

Department of Physics,

Loughborough University,

Loughborough LE11 3TU, United Kingdom

Abstract

The long-range Fröhlich electron-phonon interaction has been identified as the most essential for pairing in high-temperature superconductors owing to poor screening, as is now confirmed by optical, isotope substitution, recent photoemission and some other measurements. I argue that low energy physics in cuprate superconductors is that of superlight small bipolarons, which are real-space hole pairs dressed by phonons in doped charge-transfer Mott insulators. They are itinerant quasiparticles existing in the Bloch states at low temperatures as also confirmed by continuous-time quantum Monte-Carlo algorithm (CTQMC) fully taking into account realistic Coulomb and long-range Fröhlich interactions. Here I suggest that a parameter-free evaluation of T_c, unusual upper critical fields, the normal state Nernst effect, diamagnetism, the Hall-Lorenz numbers and giant proximity effects strongly support the three-dimensional (3D) Bose-Einstein condensation of mobile small bipolarons with zero off-diagonal order parameter above the resistive critical temperature T_c at variance with phase fluctuation scenarios of cuprates.

I.   INTRODUCTION: ESSENTIAL PAIRING INTERACTION IN CUPRATES

Although high-temperature superconductivity (HTS) has not yet been targeted as '*the shame and despair of theoretical physics*', - a label attributed to low-temperature superconductivity during the first half-century after its discovery - controversy of current theoretical constructions has led many researchers to say that there is no theory of HTS and no progress in understanding the phenomenon. A significant fraction of theoretical research in the field has suggested that the interaction in novel superconductors is essentially repulsive and unretarded, and it could provide high T_c without phonons. Indeed strong onsite repulsive correlations (Hubbard U) are essential in shaping the insulating state of undoped (parent) compounds. Different from conventional band-structure insulators with completely filled and empty Bloch bands, the Mott insulator arises from a potentially metallic half-filled band as a result of the Coulomb blockade of electron tunnelling to neighboring sites [1]. However, the Hubbard U model shares an inherent difficulty in determining the order when the Mott-Hubbard insulator is doped. While some groups have claimed that it describes high-T_c superconductivity at finite doping, other authors could not find any superconducting instability. Therefore it has been concluded that models of this kind are highly conflicting and confuse the issue by exaggerating the magnetism rather than clarifying it [2].

Here I discuss a multi-polaron approach to the problem based on the bipolaronic extension of the BCS theory to the strong-coupling regime [3]. Attractive electron correlations, prerequisite to any superconductivity, are caused by an almost unretarted electron-phonon (e-ph) interaction sufficient to overcome the direct Coulomb repulsion in this regime. Low energy physics is that of small polarons and bipolarons, which are real-space electron (hole) pairs dressed by phonons. They are itinerant quasiparticles existing in the Bloch states at temperatures below the characteristic phonon frequency. Since there is almost no retardation (i.e. no Tolmachev-Morel-Anderson logarithm) reducing the Coulomb repulsion, e-ph interactions should be relatively strong to overcome the direct Coulomb repulsion, so carriers *must* be polaronic to form pairs in novel superconductors.

In our approach to cuprate superconductors we take the view that cuprates and related transition metal oxides are charge-transfer Mott-Hubbard insulators at *any* relevant level of doping [3]. The one-particle density-of-states (DOS) of cuprates is schematically represented by Fig.1, as it has been established in a number of site-selective experiments [4] and in
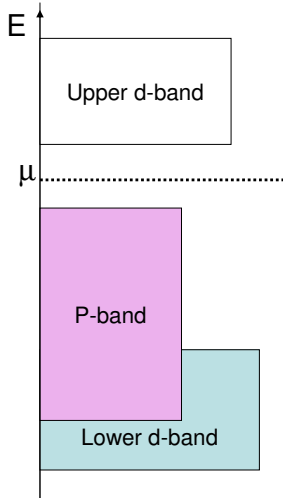
FIG. 1: DOS in cuprates. The chemical potential μ is inside the charge transfer gap as observed in the tunnelling experiments [7] because of bipolaron formation [3] . It could enter the oxygen band in overdoped cuprates, if bipolarons coexist with unpaired degenerate polarons [8].

the first-principle numerical ("LDA+U") [5] and semi-analytical cluster [6] band structure calculations properly taking into account the strong on-site repulsion.

Here d-band of the transition metal (Cu) is split into the lower and upper Hubbard bands by the on-site repulsive interaction U, while the first band to be doped is an oxygen band within the Hubbard gap. The oxygen band is completely filled in parent insulators, and doped p-holes interact with phonons and with spin fluctuations of d-band electrons. A characteristic magnetic interaction, which could be responsible for pairing is the spin-exchange interaction, $J = 4t^2/U$, of the order of 0.1 eV (here t is the hopping integral). On the other hand, a simple parameter-free estimate of the Fröhlich electron-phonon interaction (routinely neglected within the Hubbard U and/or $t - J$ approach) yields the effective attraction as high as 1 eV [3]. This estimate is obtained using the familiar expression for the polaron level shift, E_p, the high-frequency, ϵ_∞, and the static, ϵ_0, dielectric constants of the host insulator, measured experimentally [9],

$$E_p = \frac{1}{2\kappa} \int_{BZ} \frac{d^3q}{(2\pi)^3} \frac{4\pi e^2}{q^2},$$

(1)

where $\kappa^{-1} = \epsilon_\infty^{-1} - \epsilon_0^{-1}$ and the size of the integration region is the Brillouin zone (BZ). Since $\epsilon_\infty = 5$ and $\epsilon_0 = 30$ in La_2CuO_4 one obtains $E_p = 0.65$ eV. Hence the attraction, which is about $2E_p$, induced by the long-range lattice deformation in parent cuprates is one order of magnitude larger than the exchange magnetic interaction. There is virtually no screening of e-ph interactions with $c-$axis polarized optical phonons in doped cuprates because the upper limit for an out-of-plane plasmon frequency $(< 200$ cm$^{-1})$[10] is well below characteristic phonon frequencies, $\omega \approx 400$ - 1000 cm $^{-1}$. Hence the Fröhlich interaction remains the most essential pairing interaction at any doping.

Further compelling evidence for the strong e-ph interaction has come from isotope effects [11], more recent high resolution angle resolved photoemission spectroscopies (ARPES) [12], and a number of earlier optical [13, 14, 15, 16] and neutron-scattering [17] studies of cuprates. The strong coupling with optical phonons, unambiguously established in all high-temperature superconductors, transforms holes into lattice mobile polarons and mobile superconducting bipolarons as has been proposed [18, 19] prior the discovery [20, 21].

When the e-ph interaction binds holes into intersite oxygen bipolarons [3], the chemical potential remains pinned inside the charge transfer gap. It is found at a half of the bipolaron binding energy, Fig.1, above the oxygen band edge shifted by the polaron level shift E_p, as clearly observed in the tunnelling experiments by Bozovic et al. in optimally doped $La_{1.85}Sr_{0.15}CuO_4$ [7]. The bipolaron binding energy as well as the singlet-triplet bipolaron exchange energy (section 3) are thought to be the origin of normal state charge and spin pseudogaps, respectively, as has been proposed by us [22] and later found experimentally [23]. In overdoped samples carriers screen part of the e-ph interaction with low frequency phonons. Hence, the bipolaron binding energy decreases [24] and the hole bandwidth increases with doping. As a result, the chemical potential could enter the oxygen band in overdoped samples because of an overlap of the bipolaron and polaron bands, so a Fermi-level crossing could be seen in ARPPES at overdoping where mobile bipolarons coexist with degenerate polarons [8].

II. THE "FRÖHLICH-COULOMB" MODEL (FCM)

A. Canonically transformed Hamiltonian

Experimental facts tell us that any realistic description of high temperature superconductivity should treat the long-range Coulomb and *unscreened* e-ph interactions on an equal footing. In the past decade we have developed a "Fröhlich-Coulomb" model (FCM) [3, 25, 26] to deal with the strong long-range Coulomb and the strong long-range e-ph interactions in cuprates and other related compounds. The model Hamiltonian explicitly includes a long-range electron-phonon and the Coulomb interactions as well as the kinetic and deformation energies. The implicitly present large Hubbard U term prohibits double occupancy and removes the need to distinguish fermionic spins since the exchange interaction is negligible compared with the direct Coulomb and the electron-phonon interactions.

Introducing fermionic, $c_{\mathbf{n}}$, and phononic, $d_{\mathbf{m}\alpha}$, operators the Hamiltonian of the model is written as

$$
\begin{aligned}
H = & -\sum_{\mathbf{n} \neq \mathbf{n}'} \left[T(\mathbf{n} - \mathbf{n}') c_{\mathbf{n}}^{\dagger} c_{\mathbf{n}'} - \frac{1}{2} V_c(\mathbf{n} - \mathbf{n}') c_{\mathbf{n}}^{\dagger} c_{\mathbf{n}} c_{\mathbf{n}'}^{\dagger} c_{\mathbf{n}'} \right] \\
& - \sum_{\alpha, \mathbf{n}\mathbf{m}} \omega_\alpha g_\alpha(\mathbf{m} - \mathbf{n}) (\mathbf{e}_\alpha \cdot \mathbf{u}_{\mathbf{m}-\mathbf{n}}) c_{\mathbf{n}}^{\dagger} c_{\mathbf{n}} (d_{\mathbf{m}\alpha}^{\dagger} + d_{\mathbf{m}\alpha}) \\
& + \sum_{\mathbf{m}\alpha} \omega_\alpha \left(d_{\mathbf{m}\alpha}^{\dagger} d_{\mathbf{m}\alpha} + 1/2 \right),
\end{aligned}
\tag{2}
$$

where $T(\mathbf{n})$ is the hopping integral in a rigid lattice, $\mathbf{e}_\alpha$ is the polarization vector of the αth vibration coordinate, $\mathbf{u}_{\mathbf{m}-\mathbf{n}} \equiv (\mathbf{m} - \mathbf{n})/|\mathbf{m} - \mathbf{n}|$ is the unit vector in the direction from electron $\mathbf{n}$ to ion $\mathbf{m}$, $g_\alpha(\mathbf{m} - \mathbf{n})$ is the dimensionless e-ph coupling function, and $V_c(\mathbf{n} - \mathbf{n}')$ is the inter-site Coulomb repulsion. $g_\alpha(\mathbf{m} - \mathbf{n})$ is proportional to the *force* $f_{\mathbf{m}}(\mathbf{n})$ acting between the electron on site $\mathbf{n}$ and the ion on $\mathbf{m}$. For simplicity, we assume that all the phonon modes are non-dispersive with the frequency ω_α, and include spin in the definition of $\mathbf{n}$. We also use $\hbar = k_B = c = 1$.

The phonon frequency dispersion can be readily included in the definition of all essential physical quantities such as the polaron level shift, mass and the polaron-polaron interaction using the quasi-momentum representation for phonons [3]. Generally it leads to a lighter polaron compared with the nondispersive approximation. For example, comprehensive studies of the molecular Holstein model, in which the dispersive features of the phonon spectrum

are taken into account, found much lower values of the polaron mass compared with the non-dispersive model [27].

If the electron-phonon interaction is strong, i.e. the conventional e-ph coupling constant of the BCS theory is large, $\lambda > 1$, then the weak-coupling BCS [28] and the intermediate-coupling Migdal-Eliashberg [29, 30] approaches cannot be applied [31]. Nevertheless the Hamiltonian, Eq.(2), can be solved analytically using the "$1/\lambda$" multi-polaron expansion technique [3], if $\lambda = E_p/zT(a) > 1$. Here the polaron level shift is

$$E_p = \sum_{\mathbf{n}\alpha} \omega_\alpha g_\alpha^2(\mathbf{n})(\mathbf{e}_\alpha \cdot \mathbf{u_n})^2, \tag{3}$$

and $zT(a)$ is about the half-bandwidth in a rigid lattice. The model shows a rich phase diagram depending on the ratio of the inter-site Coulomb repulsion V_c and the polaron level shift E_p [26]. The ground state of FCM is a *polaronic* Fermi liquid when the Coulomb repulsion is large, a *bipolaronic* high-temperature superconductor at intermediate Coulomb repulsions, and a charge-segregated insulator if the repulsion is weak. FCM predicts *superlight* polarons and bipolarons in cuprates with a remarkably high superconducting critical temperature. Cuprate bipolarons are relatively light because they are *inter-site* rather than *on-site* pairs due to the strong on-site repulsion, and because mainly c-axis polarized optical phonons are responsible for the in-plane mass renormalization. The relatively small mass renormalization of polaronic and bipolaronic carries in FCM has been confirmed numerically using the exact Quantum Monte Carlo (QMC) [32, 33], cluster diagonalization [34] and variational [35] algorithms.

The "$1/\lambda$" expansion technique is based on the fact, known for a long time, that there is an analytical exact solution of a *single* polaron problem in the strong-coupling limit $\lambda \to \infty$. Following Lang and Firsov [36] we apply the canonical transformation e^S diagonalising the Hamiltonian, Eq.(2). The diagonalisation is exact, if $T(\mathbf{m}) = 0$ (or $\lambda = \infty$). In the Wannier representation for electrons and phonons,

$$S = \sum_{\mathbf{m}\neq\mathbf{n},\alpha} g_\alpha(\mathbf{m} - \mathbf{n})(\mathbf{e}_\alpha \cdot \mathbf{u_{m-n}})c_\mathbf{n}^\dagger c_\mathbf{n}(d_{\mathbf{m}\alpha}^\dagger - d_{\mathbf{m}\alpha}).$$

The transformed Hamiltonian is

$$\begin{aligned}
\tilde{H} &= e^{-S}He^S = -\sum_{\mathbf{n}\neq\mathbf{n}'} \hat{\sigma}_{\mathbf{n}\mathbf{n}'}c_\mathbf{n}^\dagger c_{\mathbf{n}'} + \omega\sum_{\mathbf{m}\alpha}\left(d_{\mathbf{m}\alpha}^\dagger d_{\mathbf{m}\alpha} + \frac{1}{2}\right) + \\
&\quad \frac{1}{2}\sum_{\mathbf{n}\neq\mathbf{n}'} v(\mathbf{n} - \mathbf{n}')c_\mathbf{n}^\dagger c_\mathbf{n} c_{\mathbf{n}'}^\dagger c_{\mathbf{n}'} - E_p\sum_\mathbf{n} c_\mathbf{n}^\dagger c_\mathbf{n},
\end{aligned} \tag{4}$$

where for simplicity we take $\omega_\alpha = \omega$. The last term describes the energy gained by polarons due to the e-ph interaction. The third term on the right-hand side is the polaron-polaron interaction,

$$v(\mathbf{n} - \mathbf{n'}) = V_c(\mathbf{n} - \mathbf{n'}) - V_{ph}(\mathbf{n} - \mathbf{n'}), \tag{5}$$

where

$$V_{ph}(\mathbf{n} - \mathbf{n'}) = 2\omega \sum_{\mathbf{m},\alpha} g_\alpha(\mathbf{m} - \mathbf{n}) g_\alpha(\mathbf{m} - \mathbf{n'}) \times$$
$$(\mathbf{e}_\alpha \cdot \mathbf{u}_{\mathbf{m}-\mathbf{n}})(\mathbf{e}_\alpha \cdot \mathbf{u}_{\mathbf{m}-\mathbf{n'}}).$$

The phonon-induced interaction V_{ph} is due to displacements of common ions caused by two electrons. Finally, the transformed hopping operator $\hat{\sigma}_{\mathbf{nn'}}$ is given by

$$\hat{\sigma}_{\mathbf{nn'}} = T(\mathbf{n} - \mathbf{n'}) \exp\left[\sum_{\mathbf{m},\alpha} [g_\alpha(\mathbf{m} - \mathbf{n})(\mathbf{e}_\alpha \cdot \mathbf{u}_{\mathbf{m}-\mathbf{n}}) \right. \tag{6}$$
$$\left. - g_\alpha(\mathbf{m} - \mathbf{n'})(\mathbf{e}_\alpha \cdot \mathbf{u}_{\mathbf{m}-\mathbf{n'}})] (d_{\mathbf{m}\alpha}^\dagger - d_{\mathbf{m}\alpha}) \right].$$

This term is a perturbation at large λ. It accounts for the polaron and *bipolaron* tunnelling and high temperature superconductivity [3]. In particular crystal structures like perovskites, a bipolaron tunnneling could appear already in the first order in $T(\mathbf{n})$ (see below), so that $\hat{\sigma}_{\mathbf{nn'}}$ can be averaged over phonon vacuum, if the temperature is low enough, $T \ll \omega$. The result is

$$t(\mathbf{n} - \mathbf{n'}) \equiv \langle\langle \hat{\sigma}_{\mathbf{nn'}} \rangle\rangle_{ph} = T(\mathbf{n} - \mathbf{n'}) \exp[-g^2(\mathbf{n} - \mathbf{n'})], \tag{7}$$

where

$$g^2(\mathbf{n} - \mathbf{n'}) = \sum_{\mathbf{m},\alpha} g_\alpha(\mathbf{m} - \mathbf{n})(\mathbf{e}_\alpha \cdot \mathbf{u}_{\mathbf{m}-\mathbf{n}}) \times$$
$$[g_\alpha(\mathbf{m} - \mathbf{n})(\mathbf{e}_\alpha \cdot \mathbf{u}_{\mathbf{m}-\mathbf{n}}) - g_\alpha(\mathbf{m} - \mathbf{n'})(\mathbf{e}_\alpha \cdot \mathbf{u}_{\mathbf{m}-\mathbf{n'}})].$$

By comparing Eqs.(7) and Eqs.(3,5), the bandwidth renormalization exponent can be expressed via E_p and V_{ph} as follows

$$g^2(\mathbf{n} - \mathbf{n'}) = \frac{1}{\omega} \left[E_p - \frac{1}{2} V_{ph}(\mathbf{n} - \mathbf{n'}) \right]. \tag{8}$$

In zero order with respect to the hopping the Hamiltonian, Eq.(4) describes localised polarons and independent phonons, which are vibrations of ions around new equilibrium positions depending on the polaron occupation numbers. The phonon frequencies remain
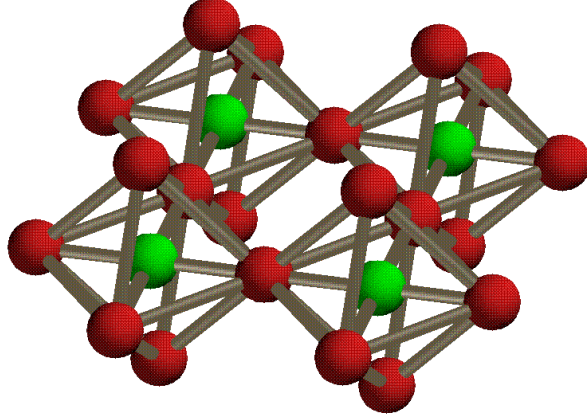
FIG. 2: Simplified model of the copper-oxygen perovskite layer [26].

unchanged in this limit. The middle of the electron band falls by the polaron level-shift E_p due to a potential well created by lattice deformation. The finite hopping term leads to the polaron tunnelling because of degeneracy of the zero order Hamiltonian with respect to site positions of the polaron.

B. Superlight small bipolarons in FCM: root to room temperature superconductivity

Now let us consider in-plane bipolarons in a two-dimensional lattice of ideal octahedra that can be regarded as a simplified model of the copper-oxygen perovskite layer, Fig.2 [26]. The lattice period is $a = 1$ and the distance between the apical sites and the central plane is $h = a/2 = 0.5$. For mathematical transperancy we assume that all in-plane atoms, both copper and oxygen, are static but apex oxygens are independent three-dimensional isotropic harmonic oscillators.

Due to poor screening, the hole-apex interaction is purely coulombic,

$$g_\alpha(\mathbf{m} - \mathbf{n}) = \frac{\kappa_\alpha}{|\mathbf{m} - \mathbf{n}|^2},$$

where $\alpha = x, y, z$. To account for the experimental fact that z-polarized phonons couple to the holes stronger than others [16], we choose $\kappa_x = \kappa_y = \kappa_z/\sqrt{2}$. The direct hole-hole repulsion is

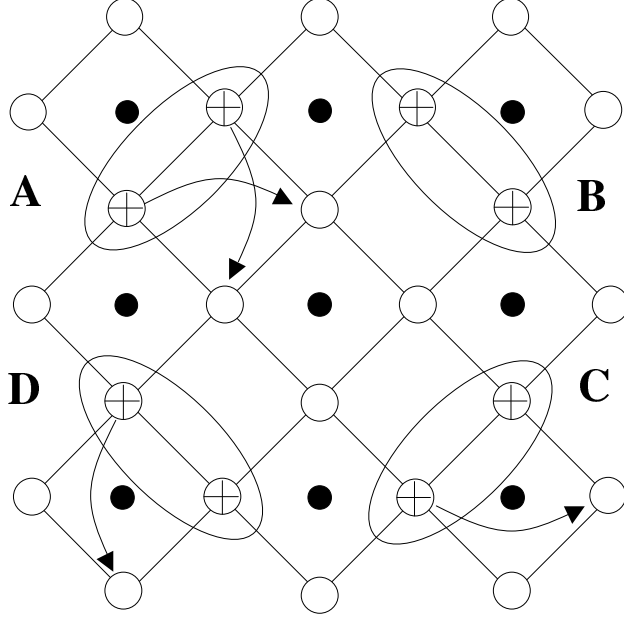$$V_c(\mathbf{n} - \mathbf{n}') = \frac{V_c}{\sqrt{2}|\mathbf{n} - \mathbf{n}'|}$$

8

FIG. 3: Four degenerate in-plane bipolaron configurations A, B, C, and D . Some single-polaron hoppings are indicated by arrows [26].

so that the repulsion between two holes in the nearest neighbour (NN) configuration is V_c. We also include the bare NN hopping T_{NN}, the next nearest neighbour (NNN) hopping across copper T_{NNN} and the NNN hopping between the pyramids T'_{NNN}.

The polaron shift is given by the lattice sum Eq.(3), which after summation over polarizations yields

$$E_p = 2\kappa_x^2\omega_0 \sum_{\mathbf{m}} \left(\frac{1}{|\mathbf{m} - \mathbf{n}|^4} + \frac{h^2}{|\mathbf{m} - \mathbf{n}|^6} \right) = 31.15\kappa_x^2\omega_0, \tag{9}$$

where the factor 2 accounts for two layers of apical sites. For reference, the Cartesian coordinates are $\mathbf{n} = (n_x + 1/2, n_y + 1/2, 0)$, $\mathbf{m} = (m_x, m_y, h)$, and n_x, n_y, m_x, m_y are integers. The polaron-polaron attraction is

$$V_{ph}(\mathbf{n} - \mathbf{n}') = 4\omega\kappa_x^2 \sum_{\mathbf{m}} \frac{h^2 + (\mathbf{m} - \mathbf{n}') \cdot (\mathbf{m} - \mathbf{n})}{|\mathbf{m} - \mathbf{n}'|^3|\mathbf{m} - \mathbf{n}|^3}. \tag{10}$$

Performing the lattice summations for the NN, NNN, and NNN' configurations one finds $V_{ph} = 1.23\,E_p$, $0.80\,E_p$, and $0.82\,E_p$, respectively. As a result, we obtain a net inter-polaron interaction as $v_{NN} = V_c - 1.23\,E_p$, $v_{NNN} = \frac{V_c}{\sqrt{2}} - 0.80\,E_p$, $v'_{NNN} = \frac{V_c}{\sqrt{2}} - 0.82\,E_p$, and the mass renormalization exponents as $g_{NN}^2 = 0.38(E_p/\omega)$, $g_{NNN}^2 = 0.60(E_p/\omega)$ and $(g'_{NNN})^2 = 0.59(E_p/\omega)$.

9

Let us now discuss different regimes of the model. At $V_c > 1.23\,E_p$, no bipolarons are formed and the system is a polaronic Fermi liquid. Polarons tunnel in the *square* lattice with $t = T_{NN} \exp(-0.38 E_p/\omega)$ and $t' = T_{NNN} \exp(-0.60 E_p/\omega)$ for NN and NNN hoppings, respectively. Since $g_{NNN}^2 \approx (g'_{NNN})^2$ one can neglect the difference between NNN hoppings within and between the octahedra. A single polaron spectrum is therefore

$$E_1(\mathbf{k}) = -E_p - 2t'[\cos k_x + \cos k_y] - 4t \cos(k_x/2) \cos(k_y/2). \tag{11}$$

The polaron mass is $m^* = 1/(t + 2t')$. Since in general $t > t'$, the mass is mostly determined by the NN hopping amplitude t.

If $V_c < 1.23\,E_p$ then intersite NN bipolarons form. The bipolarons tunnel in the plane via four resonating (degenerate) configurations A, B, C, and D, as shown in Fig.3. In the first order of the renormalised hopping integral, one should retain only these lowest energy configurations and discard all the processes that involve configurations with higher energies. The result of such a projection is the bipolaron Hamiltonian

$$
\begin{aligned}
H_b = {}& (V_c - 3.23\,E_p) \sum_{\mathbf{l}} [A_{\mathbf{l}}^\dagger A_{\mathbf{l}} + B_{\mathbf{l}}^\dagger B_{\mathbf{l}} + C_{\mathbf{l}}^\dagger C_{\mathbf{l}} + D_{\mathbf{l}}^\dagger D_{\mathbf{l}}] \\
& -t' \sum_{\mathbf{l}} [A_{\mathbf{l}}^\dagger B_{\mathbf{l}} + B_{\mathbf{l}}^\dagger C_{\mathbf{l}} + C_{\mathbf{l}}^\dagger D_{\mathbf{l}} + D_{\mathbf{l}}^\dagger A_{\mathbf{l}} + H.c.] \\
& -t' \sum_{\mathbf{n}} [A_{\mathbf{l}-\mathbf{x}}^\dagger B_{\mathbf{l}} + B_{\mathbf{l}+\mathbf{y}}^\dagger C_{\mathbf{l}} + C_{\mathbf{l}+\mathbf{x}}^\dagger D_{\mathbf{l}} + D_{\mathbf{l}-\mathbf{y}}^\dagger A_{\mathbf{l}} + H.c.],
\end{aligned}
\tag{12}
$$

where $\mathbf{l}$ numbers octahedra rather than individual sites, $\mathbf{x} = (1,0)$, and $\mathbf{y} = (0,1)$. A Fourier transformation and diagonalization of a 4×4 matrix yields the bipolaron spectrum:

$$E_2(\mathbf{K}) = V_c - 3.23 E_p \pm 2t'[\cos(K_x/2) \pm \cos(K_y/2)]. \tag{13}$$

There are four bipolaronic subbands combined in the band of the width $8t'$. The effective mass of the lowest band is $m^{**} = 2/t'$. The bipolaron binding energy is $\Delta \approx 1.23 E_p - V_c$. Inter-site bipolarons already move in the *first* order of the single polaron hopping. This remarkable property is entirely due to the strong on-site repulsion and long-range electron-phonon interactions that leads to a non-trivial connectivity of the lattice. This fact combines with a weak renormalization of t' yielding a *superlight* bipolaron with the mass $m^{**} \propto \exp(0.60\,E_p/\omega)$. We recall that in the Holstein model $m^{**} \propto \exp(2E_p/\omega)$ [18]. Thus the mass of the Fröhlich bipolaron in the perovskite layer scales approximately as a *cubic root* of that of the Holstein bipolaron.

At even stronger e-ph interaction, $V_c < 1.16E_p$, NNN bipolarons become stable. More importantly, holes can now form 3- and 4-particle clusters. The dominance of the potential energy over kinetic in the transformed Hamiltonian enables us to readily investigate these many-polaron cases. Three holes placed within one oxygen square have four degenerate states with the energy $2(V_c - 1.23E_p) + V_c/\sqrt{2} - 0.80E_p$. The first-order polaron hopping processes mix the states resulting in a ground state linear combination with the energy $E_3 = 2.71V_c - 3.26E_p - \sqrt{4t^2 + t'^2}$. It is essential that between the squares such triads could move only in higher orders of polaron hopping. In the first order, they are immobile. A cluster of four holes has only one state within a square of oxygen atoms. Its energy is $E_4 = 4(V_c - 1.23E_p) + 2(V_c/\sqrt{2} - 0.80E_p) = 5.41V_c - 6.52E_p$. This cluster, as well as all bigger ones, are also immobile in the first order of polaron hopping. We would like to stress that at distances much larger than the lattice constant the polaron-polaron interaction is always repulsive, and the formation of infinite clusters, stripes or strings is prohibited [37]. Hence the long-range Fröhlich interaction combined with Coulomb repulsion might cause clustering of polarons into finite-size quasi-metallic mesoscopic textures. However analytical [37] and QMC [38] studies of mesoscopic textures with lattice deformations and Coulomb repulsion show that pairs (i.e. bipolarons) dominate over phase separation since they effectively repel each other [3].

As shown above FCM is reduced to an extended Hubbard model with intersite attraction and suppressed double-occupancy in the limit of high phonon frequency $\omega \gtrsim T(a)$ and large on-site Coulomb repulsion. Then the Hamiltonian can be projected onto the subspace of nearest neighbor intersite bipolarons, Fig.3. In contrast with the crawler motion of on-site bipolaron, the intersite bipolaron tunnelling is a crab-like, so that its mass scales linearly with the polaron mass ($m^{**} \approx 4m^*$ on the staggered chain [26]). To study FCM for more realistic intermediate values of the electron-phonon coupling and phonon frequency the CTQMC algorithm [32, 39] has been recently extended to systems of two particles with strong electron-phonon interactions. We have solved the bipolaron problem on a staggered ladder, triangular and anisotropic hexagonal lattices from weak to strong coupling [33] in a realistic parameter range where usual limiting approximations fail. The bipolaron to polaron mass ratio has been found about 2 in the weak coupling regime ($\lambda \ll 1$) as it should be for a large bipolaron [40]. In the strong-coupling, large phonon frequency limit the mass ratio approaches 4, in agreement with strong-coupling arguments given above. In a wide region of parameter space,

we find a bipolaron/polaron mass ratio of between 2 and 4 and a bipolaron radius similar to the lattice spacing. Thus the bipolaron is small and light at the same time. Taking into account additional intersite Coulomb repulsion V_c does not change this conclusion. As V_c increases the bipolaron mass decreases but the radius remains small, at about 2 lattice spacings.

When bipolarons are small and pairs do not overlap, the pairs can form a Bose-Einstein condensate (BEC). Our CTQMC simulations show that with realistic values for the coupling constant, $\lambda \simeq 1$, and phonon frequencies, $\omega \simeq T(a)$ one can avoid overlap of pairs and get the bose-condensation temperature T_c about the room temperature. We believe that the following recipe is worth investigating to look for room-temperature superconductivity [33]: (a) The parent compound should be an ionic insulator with light ions to form high-frequency optical phonons, (b) The structure should be quasi two-dimensional to ensure poor screening of high-frequency c-axis polarized phonons, (c) A triangular lattice is required in combination with strong, on-site Coulomb repulsion to form the small superlight Crab bipolaron (d) Moderate carrier densities are required to keep the system of small bipolarons close to the dilute regime.

There are strong arguments in favor of 3D bipolaronic BEC in cuprates [3] drawn using parameter-free fitting of experimental T_c with BEC T_c [41], unusual upper critical fields [42] and the specific heat [43], and, more recently normal state diamagnetism [44], the Hall-Lorenz numbers [45, 46], the normal state Nernst effect [47, 48], and the giant proximity effect (GPE) [49] as discussed below.

III. SOME NORMAL STATE PROPERTIES OF CUPRATES IN FCM

A. Normal state Nernst effect and insulating-like in-plane resistivity

The low-energy FCM electronic structure of cuprates is shown in Fig.4 [50]. Polaronic p-holes are bound in lattice inter-site singlets (A) or in singlets and triplets (B) (if spins are included in Eq.(2)) at any temperature. Above T_c a charged bipolaronic Bose liquid is non-degenerate and below T_c phase coherence (ODLRO) of the preformed bosons sets in. The state above T_c is perfectly "normal" in the sense that the off-diagonal order parameter (i.e. the Bogoliubov-Gor'kov anomalous average $\mathcal{F}(\mathbf{r}, \mathbf{r}') = \langle \psi_\downarrow(\mathbf{r})\psi_\uparrow(\mathbf{r}') \rangle$ is zero above the
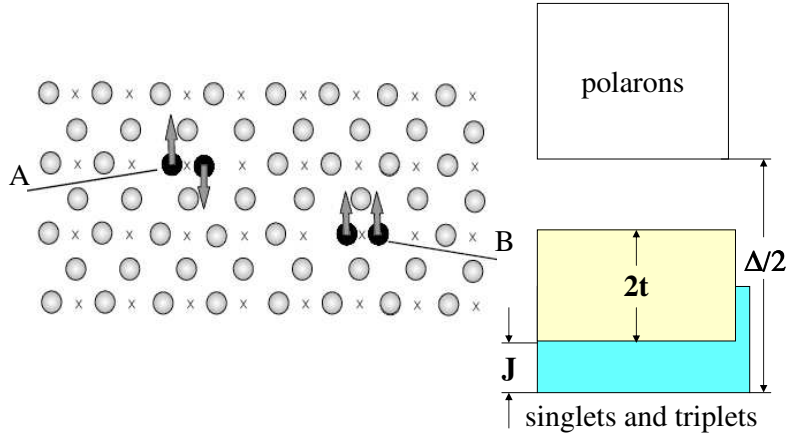
FIG. 4: Bipolaron picture of high temperature superconductors. A corresponds to a singlet oxygen intersite bipolaron, B is a triplet intersite bipolaron, Δ is the singlet bipolaron binding energy, J is the singlet-triplet exchange energy, and $2t$ is the bipolaron bandwidth [50].

resistive transition temperature T_c. Here $\psi_{\downarrow,\uparrow}(\mathbf{r})$ annihilates electrons with spin $\downarrow, \uparrow$ at point $\mathbf{r}$.

In contrast with our bipolaronic (and with BCS) theory a significant fraction of research in the field of cuprate superconductors suggests a so-called phase fluctuation scenario, where $\mathcal{F}(\mathbf{r}, \mathbf{r}')$ remains nonzero well above T_c. I believe that the phase fluctuation scenario is impossible to reconcile with the extremely sharp resistive transitions at T_c in high-quality underdoped, optimally doped and overdoped cuprates. For example, the in-plane and out-of-plane resistivity of $Bi - 2212$, where the anomalous Nernst signal has been measured [51], is perfectly "normal" above T_c, Fig.5, showing only a few percent positive or negative magnetoresistance [52], explained with bipolarons [53]. Both in-plane [54, 55, 56, 57, 58] and out-of-plane [59, 60, 61] resistive transitions of high-quality samples remain sharp in the magnetic field providing a reliable determination of the genuine $H_{c2}(T)$. The preformed Cooper-pair (or phase fluctuation) model [62] is incompatible with a great number of thermodynamic, magnetic, and kinetic measurements, which show that only holes (density x),
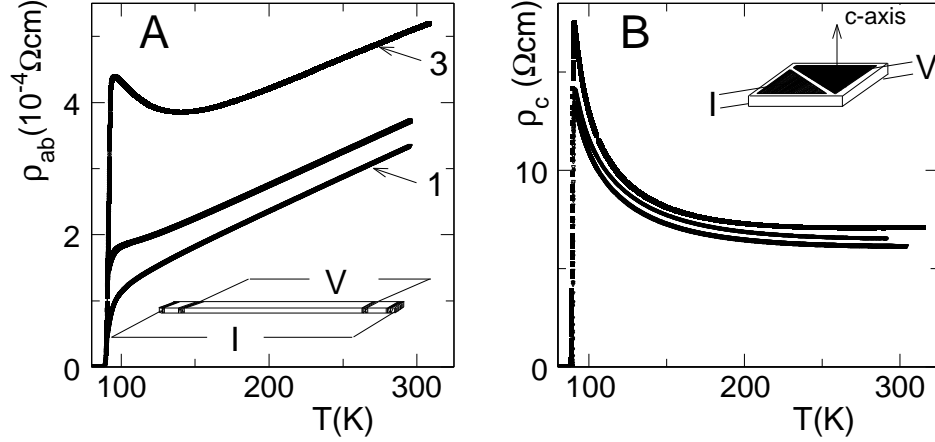
FIG. 5: In-plane (A) and out-of-plane (B) resistivity of 3 single crystals of $Bi_2Sr_2CaCu_2O_8$ [52] showing no signature of phase fluctuations above the resistive transition.

doped into a parent insulator are carriers *both* in the normal and the superconducting states of cuprates. The assumption [62] that the superfluid density x is small compared with the normal-state carrier density is also inconsistent with the theorem [63], which proves that the number of supercarriers at $T = 0K$ should be the same as the number of normal-state carriers in any clean superfluid.

Recently we have described a number of unusual normal state properties in cuprates in a different manner as perfectly normal state phenomena. In particular, the bipolaron theory accounts for the anomalously large Nernst signal, the thermopower and the insulating-like in-plane low temperature resistance [47, 48] as observed [51, 64, 65, 66].

Thermomagnetic effects appear in conductors subjected to a longitudinal temperature gradient $\nabla_x T$ in x direction and a perpendicular magnetic field in z direction. The transverse Nernst-Ettingshausen effect [67] (here the Nernst effect) is the appearance of a transverse electric field E_y in the third direction. When bipolarons are formed in the strong-coupling regime, the chemical potential is negative. It is found in the impurity band just below the mobility edge at $T > T_c$. Carriers, localised below the mobility edge contribute to the longitudinal transport together with the itinerant carriers in extended states above the mobility edge. Importantly the contribution of localised carriers of any statistics to the *transverse* transport is normally small [68] since a microscopic Hall voltage will only develop at junctions in the intersections of the percolation paths, and it is expected that these are few for the case of hopping conduction among disorder-localised states [69]. Even if this

14

contribution is not negligible, it adds to the contribution of itinerant carriers to produce a large Nernst signal, $e_y(T, B) \equiv -E_y/\nabla_x T$, while it reduces the thermopower S and the Hall angle Θ. This unusual "symmetry breaking" is completely at variance with ordinary metals where the familiar "Sondheimer" cancelation [70] makes e_y much smaller than $S \tan \Theta$ because of the electron-hole symmetry near the Fermi level. Such behaviour originates in the "sign" (or "$p - n$") anomaly of the Hall conductivity of localised carriers. The sign of their Hall effect is often *opposite* to that of the thermopower as observed in many amorphous semiconductors [68] and described theoretically [71].

The Nernst signal is expressed in terms of the kinetic coefficients σ_{ij} and α_{ij} as

$$e_y = \frac{\sigma_{xx}\alpha_{yx} - \sigma_{yx}\alpha_{xx}}{\sigma_{xx}^2 + \sigma_{xy}^2}, \tag{14}$$

where the current density is given by $j_i = \sigma_{ij}E_j + \alpha_{ij}\nabla_j T$. When the chemical potential μ is at the mobility edge, localised carriers contribute to the transport, so σ_{ij} and α_{ij} can be expressed as $\sigma_{ij}^{ext} + \sigma_{ij}^l$ and $\alpha_{ij}^{ext} + \alpha^l ij$, respectively. Since the Hall mobility of carriers localised below μ, σ_{yx}^l, has the sign opposite to that of carries in the extended states above μ, σ_{yx}^{ext}, the sign of the off-diagonal Peltier conductivity α_{yx}^l should be the same as the sign of α_{yx}^{ext}. Then neglecting the magneto-orbital effects in the resistivity (since $\Theta \ll 1$ [51]) we obtain

$$S \tan \Theta \equiv \frac{\sigma_{yx}\alpha_{xx}}{\sigma_{xx}^2 + \sigma_{xy}^2} \approx \rho(\alpha_{xx}^{ext} - |\alpha_{xx}^l|)(\Theta^{ext} - |\Theta^l|) \tag{15}$$

and

$$e_y \approx \rho(\alpha_{yx}^{ext} + |\alpha_{yx}^l|) - S \tan \Theta, \tag{16}$$

where $\Theta^{ext} \equiv \sigma_{yx}^{ext}/\sigma_{xx}$, $\Theta^l \equiv \sigma_{yx}^l/\sigma_{xx}$, and $\rho = 1/\sigma_{xx}$ is the resistivity.

Clearly the model, Eqs.(15,16) can account for a low value of $S \tan \Theta$ compared with a large value of e_y in some underdoped cuprates [51, 65] due to the sign anomaly. Even in the case when localised bosons contribute little to the conductivity their contribution to the thermopower $S = \rho(\alpha_{xx}^{ext} - |\alpha_{xx}^l|))$ could almost cancel the opposite sign contribution of itinerant carriers [47]. Indeed the longitudinal conductivity of itinerant two-dimensional bosons, $\sigma^{ext} \propto \int_0 dE E df(E)/dE$ diverges logarithmically when μ in the Bose-Einstein distribution function $f(E) = [\exp((E-\mu)/T) - 1]^{-1}$ goes to zero and the relaxation time τ is a constant. At the same time $\alpha_{xx}^{ext} \propto \int_0 dE E(E-\mu)df(E)/dE$ remains finite, and it could have the magnitude comparable with α_{xx}^l. Statistics of bipolarons gradually changes from Bose
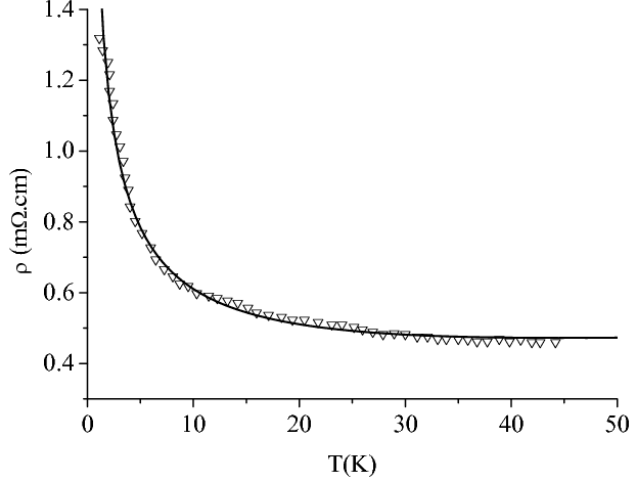
FIG. 6: Normal state in-plane resistivity of underdoped La$_{1.94}$ Sr$_{0.06}$CuO$_4$ (triangles [64]) as revealed in the field $B = 12$ Tesla and compared with the bipolaron theory, Eq.(19) (solid line).

to Fermi statistics with lowering energy across the mobility edge because of the Coulomb repulsion of bosons in localised states [72]. Hence one can use the same expansion near the mobility edge as in ordinary amorphous semiconductors to obtain the familiar textbook result $S = S_0 T$ with a constant S_0 at low temperatures [73]. The model becomes particularly simple, if we neglect the localised carrier contribution to ρ, Θ and α_{xy}, and take into account that $\alpha_{xy}^{ext} \propto B/\rho^2$ and $\Theta^{ext} \propto B/\rho$ in the Boltzmann theory. Then Eqs.(15,16) yield

$$S \tan \Theta \propto T/\rho \qquad (17)$$

and

$$e_y(T, B) \propto (1 - T/T_1)/\rho. \qquad (18)$$

According to our earlier suggestion [74] the insulating-like low-temperature dependence of $\rho(T)$ in underdoped cuprates originates from the elastic scattering of nondegenerate itinerant carriers off charged impurities. We assume here that the carrier density is temperature independent at very low temperatures. The relaxation time of nondegenerate carriers depends on temperature as $\tau \propto T^{-1/2}$ for scattering off short-range deep potential wells, and as $T^{1/2}$ for very shallow wells [74]. Combining both scattering rates we obtain

$$\rho = \rho_0[(T/T_2)^{1/2} + (T_2/T)^{1/2}]. \qquad (19)$$

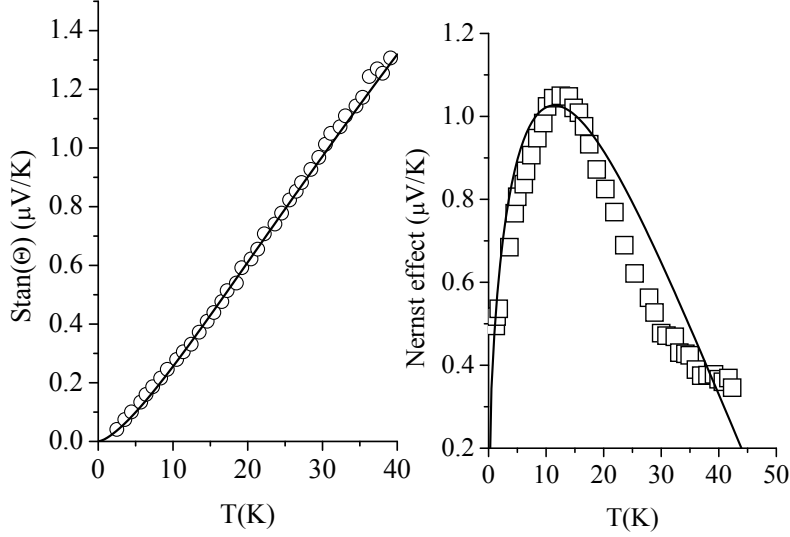Eq.(19) with $\rho_0 = 0.236$ mΩ·cm and $T_2 = 44.6$K fits extremely well the experimental

16

FIG. 7: $S \tan \Theta$ (circles [65]) and the Nernst effect e_y (squares [64]) of underdoped $La_{1.94}$ $Sr_{0.06}CuO_4$ at $B = 12$ Tesla compared with the bipolaron theory, Eqs.(20,21) (solid lines) [48].

insulating-like normal state resistivity of underdoped $La_{1.94}$ $Sr_{0.06}CuO_4$ in the whole low-temperature range from 2K up to 50K, Fig.6, as revealed in the field $B = 12$ Tesla [64, 65]. Another high quality fit can be obtained combining the Brooks-Herring formula for the 3D scattering off screened charged impurities, as proposed in Ref.[75] for almost undoped $LSCO$, or the Coulomb scattering in 2D ($\tau \propto T$) and a temperature independent scattering rate off neutral impurities with the carrier exchange [76] similar to the scattering of slow electrons by hydrogen atoms in three dimensions. Hence the scale T_2, which determines the crossover toward an insulating behavior, depends on the relative strength of two scattering mechanisms. Importantly our expressions (17,18) for $S \tan \Theta$ and e_y do not depend on the particular scattering mechanism. Taking into account the excellent fit of Eq.(19) to the experiment, they can be parameterized as

$$S \tan \Theta = e_0 \frac{(T/T_2)^{3/2}}{1 + T/T_2}, \tag{20}$$

and

$$e_y(T, B) = e_0 \frac{(T_1 - T)(T/T_2)^{1/2}}{T_2 + T}, \tag{21}$$

where T_1 and e_0 are temperature independent.

In spite of all simplifications, the model describes remarkably well both $S \tan \Theta$ and e_y, Fig.7, measured in $La_{1.94}$ $Sr_{0.06}CuO_4$ with a *single* fitting parameter, $T_1 = 50K$ using the

experimental $\rho(T)$. The constant $e_0 = 2.95$ μV/K scales the magnitudes of $S \tan \Theta$ and e_y. The magnetic field $B = 12$ Tesla destroys the superconducting state of the low-doped $La_{1.94}$ $Sr_{0.06}CuO_4$ down to 2K, Fig.6, so any residual superconducting order above 2K is clearly ruled out, while the Nernst signal, Fig.7, is remarkably large. The coexistence of the large Nernst signal and a nonmetallic resistivity is in sharp disagreement with the vortex scenario, but in agreement with our model. Taking into account the field dependence of the conductivity of localised carriers, the phonon-drug effect, and their contribution to the transverse magnetotransport can well describe the magnetic field dependence of the Nernst signal [47] and improve the fit in Fig.7 at the expense of the increasing number of fitting parameters.

B. Hall-Lorenz number

Recent measurements of the Righi-Leduc effect provides further evidence for real-space charged bosons preformed above T_c [45, 46]. The effect describes transverse heat flow resulting from a perpendicular temperature gradient in an external magnetic field, which is a thermal analog of the Hall effect. Using the effect the "Hall-Lorenz" electronic number, $L_H = (e/k_B)^2 \kappa_{xy}/(T\sigma_{xy})$ has been directly measured [77] in $YBa_2Cu_3O_{6.95}$ and $YBa_2Cu_3O_{6.6}$ since transverse thermal κ_{xy} and electrical σ_{xy} conductivities involve presumably only electrons. The experimental $L_H(T)$ showed a quasi-linear temperature dependence above the resistive T_c, which strongly violates the WF law. Remarkably, the measured value of L_H just above T_c turned out precisely the same as predicted by the bipolaron theory [78], $L = 0.15L_0$, where $L_0 = \pi^2/3$ is the conventional Sommerfeld value. The breakdown of the WF law revealed in the Righi-Leduc effect [77] has been explained by a temperature-dependent contribution of thermally excited single polarons to the transverse magneto-transport [45].

Surprisingly more recent measurements of the Hall-Lorenz number in single crystals of optimally doped $YBa_2Cu_3O_{6.95}$ and optimally doped and underdoped $EuBa_2Cu_3O_y$ led to an opposite conclusion [79]. The experimental L_H for these samples has turned out only weakly temperature dependent and exceeding the Sommerfeld value by more than 2 times in the whole temperature range from T_c up to the room temperature. Following an earlier claim[80] Matusiak and Wolf [79] have argued that a possible reason for such significant

difference might be that Zhang et al. [77] used different samples, one for κ_{xy} and another one for σ_{xy} measurements, which makes their results for L_H inconsistent.

Actually it has been shown [46] that there is no inconsistency in both L_H determinations. One order of magnitude difference in two independent direct measurements of the normal-state Hall-Lorenz number is consistently explained by the bipolaron theory [3]. The theory explains the huge difference in the Hall-Lorenz numbers by taking into account the difference between the in-plane resistivity of detwinned [77] and twinned [79] single crystals. It fits well the observed $L_H(T)$s and explains a sharp Hall-number maximum [79] observed in the normal state of underdoped cuprates.

In the presence of the electric field $\mathbf{E}$, the temperature gradient $\boldsymbol{\nabla}T$ and a weak magnetic field $\mathbf{B} \| \mathbf{z} \perp \mathbf{E}$ and $\boldsymbol{\nabla}T$, the electrical currents in x, y directions are given by

$$
\begin{aligned}
j_x =& a_{xx}\nabla_x(\mu - 2e\phi) + a_{xy}\nabla_y(\mu - 2e\phi) \\
&+ b_{xx}\nabla_x T + b_{xy}\nabla_y T, \\
j_y =& a_{yy}\nabla_y(\mu - 2e\phi) + a_{yx}\nabla_x(\mu - 2e\phi) \\
&+ b_{yy}\nabla_y T + b_{yx}\nabla_x T,
\end{aligned}
$$

$$(22)$$

and the thermal currents are:

$$
\begin{aligned}
w_x =& c_{xx}\nabla_x(\mu - 2e\phi) + c_{xy}\nabla_y(\mu - 2e\phi) \\
&+ d_{xx}\nabla_x T + d_{xy}\nabla_y T \\
w_y =& c_{yy}\nabla_y(\mu - 2e\phi) + c_{yx}\nabla_x(\mu - 2e\phi) \\
&+ d_{yy}\nabla_y T + d_{yx}\nabla_x T.
\end{aligned}
$$

$$(23)$$

Here μ and ϕ are the chemical and electric potentials.

Real phonons and (bi)polarons are well decoupled in the strong-coupling regime of the electron-phonon interaction [3] so the standard Boltzmann equation for the kinetics of renormalised carriers is applied. If we make use of the $\tau(E)-$approximation [81] the kinetic

coefficients of bipolarons are found as [45]

$$
\begin{aligned}
a_{xx}^b &= a_{yy}^b = \frac{2en_b}{m_b}\langle\tau_b\rangle, \\
a_{yx}^b &= -a_{xy}^b = \frac{2eg_bBn_b}{m_b}\langle\tau_b^2\rangle, \\
b_{xx}^b &= b_{yy}^b = \frac{2en_b}{Tm_b}\langle(E-\mu)\tau_b\rangle, \\
b_{yx}^b &= -b_{xy}^b = \frac{2eg_bBn_b}{Tm_b}\langle(E-\mu)\tau_b^2\rangle,
\end{aligned}
$$

and

$$
\begin{aligned}
c_{xx}^b &= c_{yy}^b = \frac{n_b}{m_b}\langle(E+2e\phi)\tau_b\rangle, \\
c_{yx}^b &= c_{xy}^b \frac{g_bBn_b}{m_b}\langle(E+2e\phi)\tau_b^2\rangle, \\
d_{xx}^b &= d_{yy}^b = \frac{n_b}{Tm_b}\langle(E+2e\phi)(E-\mu)\tau_b\rangle, \\
d_{yx}^b &= -d_{xy}^b = \frac{g_bBn_b}{Tm_b}\langle(E+2e\phi)(E-\mu)\tau_b^2\rangle,
\end{aligned}
$$

where

$$
\langle Q(E)\rangle = \frac{\int_0^\infty dE\,Q(E)E D_b(E)\partial f_b/\partial E}{\int_0^\infty dE\,E D_b(E)\partial f_b/\partial E}, \tag{24}
$$

$D_b(E) \propto E^{d/2-1}$ is the density of states of a d-dimensional bipolaron spectrum, $E = K^2/(2m_b)$, $g_b = 2e/m_b$, and $f_b(E)$ is the equilibrium distribution function. Polaronic coefficients are obtained by replacing super/subscripts b for p, double elementary charge $2e$ for e and μ for $\mu/2$ in all kinetic coefficients, and m_b for $2m_p$ in a_{ij} and c_{ij}. The kinetic energy of bipolarons, E should be replaced by $E + T^*$, where $E = k^2/(2m_p)$ is the polaron kinetic energy, and T^* is half of the bipolaron binding energy (i.e. the pseudogap temperature in the theory [3]).

The in-plane resistivity, ρ, the Hall number, R_H, and the Hall-Lorenz number, L_H are expressed in terms of the kinetic coefficients as $\rho^{-1} = 2ea_{xx}$, $R_H = a_{yx}/2eB(a_{xx})^2$, and

$$
L_H = \frac{e\left[(d_{yx}a_{xx} - c_{yx}b_{xx})a_{xx} - c_{xx}(b_{xx}a_{yx} - b_{yx}a_{xx})\right]}{2Ta_{yx}a_{xx}^2}, \tag{25}
$$

respectively, where $a, b, c, d = a^p + a^b, b^p + b^b, c^p + c^b, d^p + d^b$.

The *in*-plane resistivity, the temperature-dependent paramagnetic susceptibility, and the Hall ratio have been described by the bipolaron model taking into account thermally activated single polarons [82, 83, 84, 85]. The bipolaron model has also offered a simple

explanation of c-axis transport and the anisotropy of cuprates [24, 60, 61, 84]. The crucial point is that single polarons dominate in c-axis transport at finite temperatures because they are much lighter than bipolarons in c-direction. Bipolarons can propagate across the planes only via a simultaneous two-particle tunnelling, which is much less probable than a single polaron tunnelling. However, along the planes polarons and inter-site bipolarons propagate with comparable effective masses (section 2). Hence in the mixture of nondegenerate quasi-two-dimensional (2D) bosons and thermally excited 3D fermions, only fermions contribute to c-axis transport, if the temperature is not very low, which leads to the thermally activated c-axis transport and to the huge anisotropy of cuprates [24].

We have also shown [45] that by the necessary inclusion of thermally activated polarons, the model predicts a breakdown of the WF law with the small near-linear in temperature Hall-Lorenz number, as observed experimentally by Zhang et al. [77] (see Fig.8). Let us now show that the bipolaron model describes the contrasting observations of Ref. [79] as well, if the ratio of bipolaron and polaron mobilities, $\alpha = 2\tau_b m_p/\tau_p m_b$ becomes relatively small.

Both polaronic and bipolaronic carriers are not degenerate above T_c, so the classical distribution functions, $f_b = y \exp(-E/T)$ and $f_p = y^{1/2} \exp[-(E + T^*)/T]$ are applied with $y = \exp(\mu/T)$. The chemical potential is evaluated using $2n_b + n_p = x/v_0$, where x is the number of itinerant holes in the unit cell volume v_0 not localised by disorder. The bipolaron density remains large compared with the polaron density in a wide temperature range, so that $n_b v_0 \approx x/2$ and $y \approx \pi x/(m_b a^2 T)$ for quasi-2D bipolarons. Then the atomic density of 3D polarons is $n_p v_0 = T m_p a^2 \exp(-T^*/T)(x m_p/2\pi^2 m_b)^{1/2}$ (a is the lattice constant). The ratio $\beta = n_p/2n_b$ remains small at any pseudogap temperature T^* and any relevant doping level $x > 0.05$, $\beta \approx T \exp(-T^*/T)(18 m_p/\pi^2 x m_b)^{1/2}/W \ll 1$, if the temperature T is small compared with the polaron bandwidth $W = 6/m_p a^2$. Hence, if the mobility ratio α is of the order of unity, both longitudinal and transverse in-plane magnetotransport is dominated by bipolarons, which explains a remarkably low L_H in high-quality detwinned crystals used in Ref.[77], Fig.8.

On the other hand, twinned crystals used in Ref.[79] had the in-plane resistivity several times larger than those of Ref. [77] presumably resulting from twin boundaries and long term aging. The twin boundaries and other defects are strong scatterers for slow 2D bipolarons, while lighter quasi-3D polarons are mainly scattered by real optical phonons, which
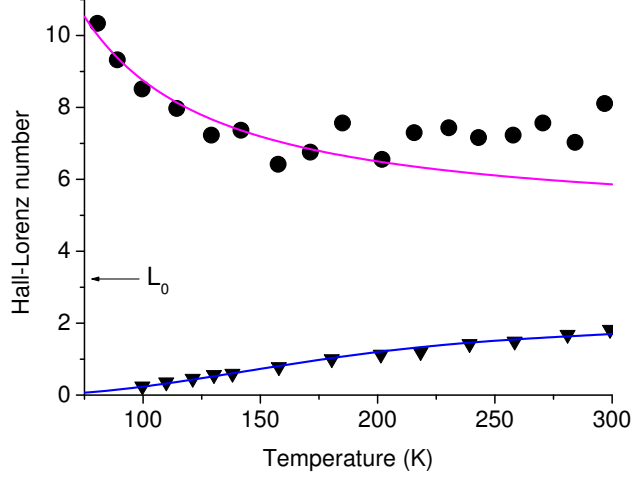
FIG. 8: The Hall-Lorenz number L_H in underdoped twinned $EuBa_2Cu_3O_{6.65}$ (circles)[79] compared with the theory, Eq.(28) when $\alpha \ll 1$(upper line), and the significantly different Hall-Lorenz number in detwinned $YBa_2Cu_3O_{6.95}$ (triangles)[77] described by the same theory [45] with a moderate value of $\alpha = 0.44$ (lower line).

are similar in all crystals. Hence one can expect that α becomes small in twinned crystals of Ref. [79]. If the condition $\alpha^2 \ll \beta$ is met, then only polarons contribute to the transverse electric and thermal magnetotransport. It explains about the same thermal Hall conductivities ($\kappa_{xy} \approx 2.5 \times 10^{-3} B$ W/Km at T=100K) dominated by polarons in both crystals of $YBa_2Cu_3O_{6.95}$ used in Ref. [77] and in Ref. [79], and at the same time a substantial difference of their electrical Hall conductivities, σ_{xy}, as bipolarons virtually do not contribute to σ_{xy} in the twinned samples.

To arrive at simple analytical results and illustrate their quantitative agreement with the experiment [79] let us assume that $\alpha^2 \ll \beta$, but $\alpha \gtrsim \beta$, and neglect an energy dependence of the transport relaxation rates of all carriers. In such conditions bipolarons do not contribute to transverse heat and electric flows, but determine the in-plane conductivity. Kinetic responses are grossly simplified as

$$\rho = \frac{m_b v_0}{2e^2 x \tau_b} \tag{26}$$

$$R_H = \frac{v_0 \beta}{e x \alpha^2} = \frac{e^3 n_p \tau_p^2}{m_p^2} \rho^2, \tag{27}$$

$$L_H = 4.75 + 3T^*/T + (T^*/T)^2. \tag{28}$$

22

As in the case of $\alpha^2 \gtrsim \beta$, discussed in Ref. [45], the recombination of a pair of polarons into bipolaronic bound states at the cold end of the sample results in the breakdown of the WF law, as described by two temperature-dependent terms in Eq.(28). The breakdown is reminiscent of the one in conventional semiconductors caused by the recombination of electron-hole pairs at the cold end [81]. However, the temperature dependence and the value of $L_H(T)$ turn out remarkably different. When $\alpha^2 \ll \beta$, The Hall-Lorenz number is more than by an order of magnitude larger than in the opposite regime, $\alpha^2 \gtrsim \beta$. It increases with temperature lowering rather than decreases fitting well the experimental observation[79] in twinned underdoped single crystals of $EuBa_2Cu_3O_{6.65}$ with $T^* = 100$K, Fig.8. Hence by varying the bipolaron to polaron mobility ratio, α, the model accounts for qualitatively different behaviours of $L_H(T)$ in twinned and detwinned cuprates.

C.   Normal state diamagnetism

A number of experiments (see, for example, [66, 86, 87, 88, 89, 90] and references therein), including torque magnetometries, showed enhanced diamagnetism above T_c, which has been explained as the fluctuation diamagnetism in quasi-2D superconducting cuprates (see, for example Ref. [88]). The data taken at relatively low magnetic fields (typically below 5 Tesla) revealed a crossing point in the magnetization $M(T, B)$ of most anisotropic cuprates (e.g. $Bi - 2212$), or in $M(T, B)/B^{1/2}$ of less anisotropic $YBCO$ [87]. The dependence of magnetization (or $M/B^{1/2}$) on the magnetic field has been shown to vanish at some characteristic temperature below T_c. However the data taken in high magnetic fields (up to 30 Tesla) have shown that the crossing point, anticipated for low-dimensional superconductors and associated with superconducting fluctuations, does not explicitly exist in magnetic fields above 5 Tesla [89].

Most surprisingly the torque magnetometery [86, 89] uncovered a diamagnetic signal somewhat above T_c which increases in magnitude with applied magnetic field. It has been linked with the Nernst signal and mobile vortexes in the normal state of cuprates [66]. However, apart from the inconsistences mentioned above, the vortex scenario of the normal-state diamagnetism is internally inconsistent. Accepting the vortex scenario and fitting the magnetization data in $Bi - 2212$ with the conventional logarithmic field dependence [66], one obtains surprisingly high upper critical fields $H_{c2} > 120$ Tesla and a very large

Ginzburg-Landau parameter, $\kappa = \lambda/\xi > 450$ even at temperatures close to T_c. The in-plane low-temperature magnetic field penetration depth is $\lambda = 200$ nm in optimally doped $Bi-2212$ (see, for example [91]). Hence the zero temperature coherence length ξ turns out to be about the lattice constant, $\xi = 0.45$nm, or even smaller. Such a small coherence length rules out the "preformed Cooper pairs" [62], since the pairs are virtually not overlapped at any size of the Fermi surface in $Bi-2212$. Moreover the magnetic field dependence of $M(T, B)$ at and above T_c is entirely inconsistent with what one expects from a vortex liquid. While $-M(B)$ decreases logarithmically at temperatures well below T_c, the experimental curves [66, 86, 89] clearly show that $-M(B)$ increases with the field at and above T_c, just opposite to what one could expect in the vortex liquid. This significant departure from the London liquid behavior clearly indicates that the vortex liquid does not appear above the resistive phase transition [86].

Some time ago we explained the anomalous diamagnetism in cuprates as the Landau normal-state diamagnetism of preformed bosons [92]. The same model predicted the unusual upper critical field [42] observed in many superconducting cuprates [54, 55, 56, 57, 58, 59]. More recently the model has been extended to high magnetic fields taking into account the magnetic pair-breaking of singlet bipolarons and the anisotropy of the energy spectrum [44]. When the magnetic field is applied perpendicular to the copper-oxygen plains the quasi-2D bipolaron energy spectrum is quantized as $E_\alpha = \omega(n + 1/2) + 2t_c[1 - \cos(K_z d)]$, where α comprises $n = 0, 1, 2, ...$ and in-plane K_x and out-of-plane K_z center-of-mass quasi-momenta, $\omega = 2eB/\sqrt{m_x^{**}m_y^{**}}$, t_c and d are the hopping integral and the lattice period perpendicular to the planes. We assume here that the spectrum consists of two degenerate branches, so-called "x" and "y" bipolarons as in the case of apex intersite pairs [25] with anisotropic in-plane bipolaron masses $m_x^{**} \equiv m$ and $m_y^{**} \approx 4m$. Expanding the Bose-Einstein distribution function in powers of $\exp[(\mu - E)/T]$ with the negative chemical potential μ one can after summation over n readily obtain the boson density

$$n_b = \frac{2eB}{\pi d} \sum_{r=1}^{\infty} I_0(2t_c r/T) \frac{\exp[(\mu - \omega/2 - 2t_c)r/T]}{1 - \exp(-\omega r/T)}, \tag{29}$$

and the magnetization,

$$M(T, B) = -n_b\mu_b + \frac{2eT}{\pi d} \sum_{r=1}^{\infty} I_0\left(\frac{2t_c r}{T}\right) \times \tag{30}$$

$$\frac{\exp[(\mu - \omega/2 - 2t_c)r/T]}{1 - \exp(-\omega r/T)}\left(\frac{1}{r} - \frac{\omega \exp(-\omega r/T)}{k_B T[1 - \exp(-\omega r/T)]}\right).$$
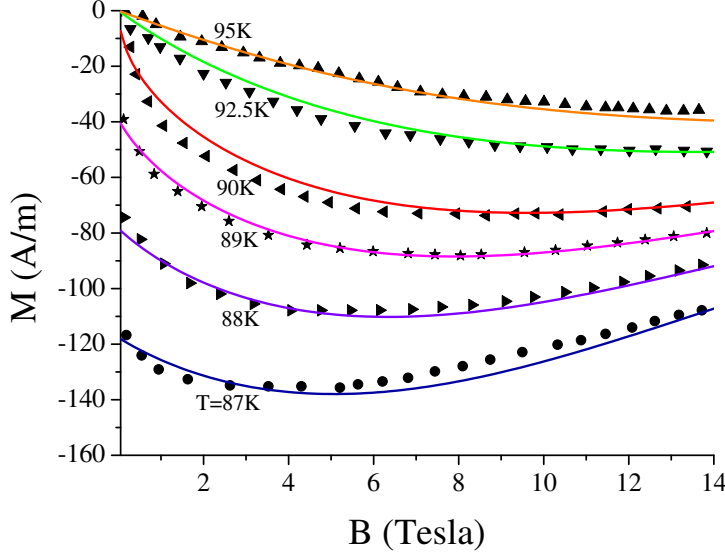
24

FIG. 9: Diamagnetism of optimally doped Bi-2212 (symbols)[66] compared with magnetization of CBG [44] near and above T_c (lines).

Here $\mu_b = e/\sqrt{m_x^{**} m_y^{**}}$ and $I_0(x)$ is the modified Bessel function. At low temperatures $T \to 0$ Schafroth's result [96] is recovered, $M(0, B) = -n_b \mu_b$. The magnetization of charged bosons is field-independent at low temperatures. At high temperatures, $T \gg T_c$ the chemical potential has a large magnitude, and we can keep only the terms with $r = 1$ in Eqs.(85,86) to obtain $M(T, B) = -n_b \mu_b \omega/(6T)$ at $T \gg T_c \gg \omega$, which is the familiar Landau orbital diamagnetism of nondegenerate carriers. Here T_c is the Bose-Einstein condensation temperature $T_c = 3.31(n_b/2)^{2/3}/(m_x^{**} m_y^{**} m_c^{**})^{1/3}$, with $m_c = 1/2|t_c|d^2$.

Comparing with experimental data one has to take into account a temperature and field depletion of singlets due to their thermal excitations into spin-split triplets and single polaron states, Fig.4. If $J < \Delta/2$, triplets mainly contribute to temperature and field dependencies of the singlet bipolaron density near T_c, $n_b(T, B) = n_c[1 - \alpha\tau - (B/B^*)^2]$. Here $\alpha = 3(2n_c t)^{-1}[J(e^{J/T_c} - 1)^{-1} - T_c \ln(1 - e^{-J/T_c})]$, $\mu_B B^* = (2T_c n_c t)^{1/2} \sinh(J/2T_c)$, $\mu_B \approx 0.93 \times 10^{-23}$ Am^2 is the Bohr magneton, n_c is the density of singlets at $T = T_c$ in zero field, $\tau = T/T_c - 1$, and $2t$ is the triplet bandwidth. A triplet contribution to diamagnetism remains negligible compared with the singlet diamagnetism if $|1 - T/T_c| \ll J/T_c$. Also bosons localised in a random potential contribute to the diamagnetism. However their contribution remains small compared with the extended carrier diamagnetism, if the localization energy

25

is large compared with T. As a result, Eq.(30) fits remarkably well the experimental curves in the critical region of optimally doped Bi-2212, Fig.9, with $n_c \mu_b = 2100 \text{A/m}$, $T_c = 90 \text{K}$, $\alpha = 0.62$ and $B^* = 56$ Tesla, which corresponds to the singlet-triplet exchange energy $J \approx 20 \text{K}$.

D. Giant proximity effect

Several groups reported that in the Josephson cuprate SNS junctions supercurrent can run through normal N-barriers thicker than 100 nm in a strong conflict with the standard theoretical picture, if the barrier is made from non-superconducting cuprates. Using an advanced molecular beam epitaxy, Bozovic et $al.$ [94] proved that this giant proximity effect (GPE) is intrinsic, rather than extrinsic caused by any inhomogeneity of the barrier. Hence GPE defies the conventional explanation, which predicts that the critical current should exponentially decay with the characteristic length of about the coherence length, which is $\xi \lesssim 1$ nm in the cuprates.

Here I show that the effect can be broadly understood as the Bose-Einstein condensate (BEC) tunnelling into a cuprate $semiconductor$. As mentioned in section 1, the chemical potential μ remains in the charge-transfer gap of doped cuprates like $La_{2-x}Sr_xCuO_4$ [7] because of bipolaron formation. The condensate wave function, $\psi(Z)$, is described by the Gross-Pitaevskii (GP) equation. In the superconducting region, $Z < 0$, near the SN boundary, Fig.10, the equation is

$$\frac{1}{2m_c^{**}} \frac{d^2\psi(Z)}{dZ^2} = [V|\psi(Z)|^2 - \mu]\psi(Z), \tag{31}$$

where V is a short-range repulsion of bosons, and m_c^{**} is the boson mass along Z. Deep inside the superconductor $|\psi(Z)|^2 = n_s$ and $\mu = V n_s$, where the condensate density n_s is about $x/2$, if the temperature is well below T_c of the superconducting electrode (the in-plane lattice constant a and the unit cell volume are taken as unity).

The normal barrier at $Z > 0$ is an underdoped cuprate semiconductor above its transition temperature, where the chemical potential μ lies below the bosonic band by some energy ϵ, Fig.10. One obtains for quasi-two dimensional bosons [3]

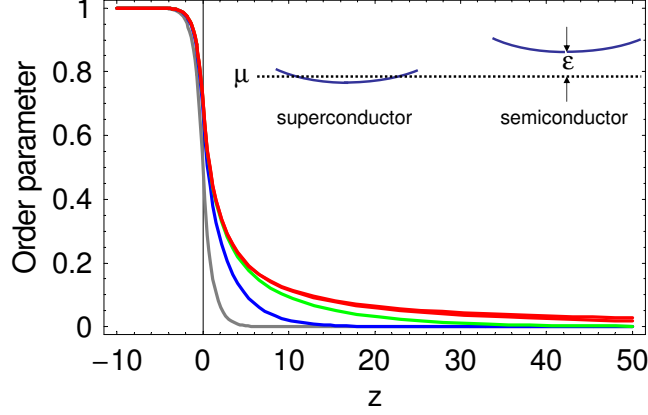$$\epsilon = -T \ln(1 - e^{-T_0/T}), \tag{32}$$

FIG. 10: BEC order parameter at the SN boundary for $\tilde{\mu} = 1.0, 0.1, 0.01$ and $\leqslant 0.001$ (upper curve).

where $T_0 = \pi x'/m^{**}$, m^{**} is the in-plane boson mass, and $x' < x$ is the doping level of the barrier. Then the GP equation in the barrier can be written as

$$\frac{1}{2m_c^{**}} \frac{d^2\psi(Z)}{dZ^2} = [V|\psi(Z)|^2 + \epsilon]\psi(Z). \tag{33}$$

Introducing the bulk coherence length, $\xi = 1/(2m_c^{**}n_s V)^{1/2}$ and dimensionless $f(z) = \psi(Z)/n_s^{1/2}$, $\tilde{\mu} = \epsilon/n_s V$, and $z = Z/\xi$ one obtains for a real $f(z)$

$$\frac{d^2 f}{dz^2} = f^3 - f, \tag{34}$$

if $z < 0$, and

$$\frac{d^2 f}{dz^2} = f^3 + \tilde{\mu} f, \tag{35}$$

if $z > 0$. These equations can be readily solved using first integrals of motion respecting the boundary conditions, $f(-\infty) = 1$, and $f(\infty) = 0$,

$$\frac{df}{dz} = -(1/2 + f^4/2 - f^2)^{1/2}, \tag{36}$$

and

$$\frac{df}{dz} = -(\tilde{\mu}f^2 + f^4/2)^{1/2}, \tag{37}$$

27

for $z < 0$ and $z > 0$, respectively. The solution in the superconducting electrode is given by

$$f(z) = \tanh\left[-2^{-1/2}z + 0.5\ln\frac{2^{1/2}(1+\tilde{\mu})^{1/2}+1}{2^{1/2}(1+\tilde{\mu})^{1/2}-1}\right]. \tag{38}$$

It decays in the close vicinity of the barrier from 1 to $f(0) = [2(1+\tilde{\mu})]^{-1/2}$ in the interval about the coherence length ξ. On the other side of the boundary, $z > 0$, it is given by

$$f(z) = \frac{(2\tilde{\mu})^{1/2}}{\sinh\{z\tilde{\mu}^{1/2} + \ln[2(\tilde{\mu}(1+\tilde{\mu}))^{1/2} + (1+4\tilde{\mu}(1+\tilde{\mu}))^{1/2}]\}}. \tag{39}$$

Its profile is shown in Fig.10. Remarkably, the order parameter penetrates into the normal layer up to the length $Z^* \approx (\tilde{\mu})^{-1/2}\xi$, which could be larger than ξ by many orders of magnitude, if $\tilde{\mu}$ is small. It is indeed the case, if the barrier layer is sufficiently doped. For example, taking $x' = 0.1$, c-axis $m_c^{**} = 2000m_e$, in-plane $m^{**} = 10m_e$ [3], $a = 0.4$ nm, and $\xi = 0.6$ nm, yields $T_0 \approx 140$ K and $(\tilde{\mu})^{-1/2} \approx 5000$ at $T = 10$K. Hence the order parameter could penetrate into the normal cuprate semiconductor up to more than a thousand coherence lengths as observed [94]. If the thickness of the barrier L is small compared with Z^*, and $(\tilde{\mu})^{1/2} \ll 1$, the order parameter decays following the power law, rather than exponentially,

$$f(z) = \frac{\sqrt{2}}{z+2}. \tag{40}$$

Hence, for $L \lesssim Z^*$, the critical current should also decay following the power law [49]. On the other hand, for an *undoped* barrier $\tilde{\mu}$ becomes larger than unity, $\tilde{\mu} \propto \ln(m^{**}T/\pi x') \to \infty$ for any finite temperature T when $x' \to 0$, and the current should exponentially decay with the characteristic length smaller that ξ, as is experimentally observed as well [7].

IV. DISCUSSION

A possibility of real-space pairing, as opposed to the Cooper pairing, has been the subject of many discussions, particularly heated over the last 20 years after the discovery of high temperature superconductivity in cuprates. The first proposal for high temperature super-conductivity, made by Ogg Jr in 1946 [95], already involved real-space pairing of individual electrons into bosonic molecules with zero total spin. This idea was further developed as a natural explanation of conventional superconductivity by Schafroth and Butler and Blatt [96]. However, with one or two exceptions, the Ogg-Schafroth picture was condemned and practically forgotten because it neither accounted quantitatively for the critical behavior of

conventional superconductors, nor did it explain the microscopic nature of attractive forces which could overcome the Coulomb repulsion between two electrons constituting a pair. The failure of the 'bosonic' picture of individual electron pairs became fully transparent when Bardeen, Cooper and Schrieffer [28] proposed that two electrons in a superconductor were indeed correlated, but at a very large distance of about 10^3 times of the average inter-electron spacing.

Highly successful for low-Tc metals and alloys the BCS theory has led many researchers to believe that novel high-temperature superconductors should also be "BCS-like". However, the Ogg-Schafroth and the BCS descriptions are actually two opposite extremes of the same electron-phonon (e-ph) interaction. Indeed by extending the BCS theory towards the strong interaction between electrons and ion vibrations, a charged Bose gas (CBG) of tightly bound small bipolarons was predicted by us [18] with a further prediction that high T_c should exist in the crossover region of the e-ph interaction strength from the BCS-like to bipolaronic superconductivity [19].

However, for very strong electron-phonon coupling, polarons become self-trapped on a single lattice site. The energy of the resulting small polaron is given as $E_p = -\lambda z T(a)$, where λ is the electron-phonon coupling constant, $T(a)$ is the hopping parameter and z is the coordination number. Expanding about the atomic limit in small $T(a)$ (which is small compared to E_p in the small polaron regime, $\lambda > 1$) the polaron mass is computed as $m^* = m_0 \exp(\gamma z \lambda / \hbar \omega)$, where ω is the frequency of Einstein phonons, m_0 is the rigid band mass on a cubic lattice, and γ is a numerical constant. For the Holstein model, which is purely site local, $\gamma = 1$. Bipolarons are on-site singlets in the Holstein model and their mass m_H^{**} appears only in the second order of $T(a)$ [18] scaling as $m_H^{**} \propto (m^*)^2$ in the limit $\hbar \omega \gg \Delta$, and as $m_H^{**} \propto (m^*)^4$ in a more realistic regime $\hbar \omega \ll \Delta$ [97]. Here $\Delta = 2E_p - U$ is the bipolaron binding energy, and U is the on-site (Hubbard) repulsion. Since the Hubbard U is about 1 eV or larger in strongly correlated materials, the electron-phonon coupling must be large to stabilize on-site bipolarons and the Holstein bipolaron mass appears very large, $m_H^{**}/m_0 > 1000$, for realistic values of phonon frequency.

This estimate led some authors to the conclusion that the formation of itinerant small polarons and bipolarons in real materials is unlikely [98], and high-temperature bipolaronic superconductivity is impossible [99]. However, one should note that the Holstein model is an extreme polaron model, and typically yields the highest possible value of the (bi)polaron

mass in the strong coupling limit. Many advanced materials with low density of free carriers and poor mobility (at least in one direction) are characterized by poor screening of high-frequency optical phonons and are more appropriately described by the long-range Fröhlich electron-phonon interaction [25]. For this interaction the parameter γ is less than 1 ($\gamma \approx 0.3$ on the square lattice and $\gamma \approx 0.2$ on the triangular lattice), reflecting the fact that in a hopping event the lattice deformation is partially pre-existent. Hence the unscreened Fröhlich electron-phonon interaction provides relatively light small polarons, which are several orders of magnitude lighter than small Holstein polarons, which is now confirmed by several numerical studies as discussed in section 2.

This unscreened Fröhlich interaction combined with on-site repulsive correlations can bind holes into superlight intersite bipolarons (section 2). Experimental evidence for exceptionally strong e-ph interactions is now so overwhelming that the bipolaronic charged bose gas [3] could be a feasible alternative to the BCS-like scenarios of cuprates. While some authors [62] have dismissed any real-space pairing, advocating a *collective* pairing into incoherent Cooper pairs in the momentum space at some high temperature $T^* > T_c$, I argue that the most likely scenario is a true 3D Bose-Einstein condensation at T_c of real-space bipolarons. Our bipolaron theory predicted such key features of cuprate superconductors as anomalous upper critical fields, spin and charge pseudogaps, and anomalous isotope effects later discovered experimentally. The theory explained normal state kinetics, high T_c values, and specific heat anomalies of cuprates (see [3] and references therein).

Here I have reviewed normal-state diamagnetism, the Nernst, thermal Hall and giant proximity effects as strong evidence for real-space pairing and 3D BEC in cuprates.

[1] N.F.Mott, *Metal-Insulator Transitions, 2nd ed* (Taylor&Francis, London 1990).

[2] R.B. Laughlin, cond-mat/0209269; B.A. Bernevig, R.B. Laughlin, and D.I. Santiago, *Phys. Rev. Lett.* **91**, 147003 (2003).

[3] A.S. Alexandrov, *Theory of Superconductivity: From Weak to Strong Coupling* (IoP Publish-

ing, Bristol and Philadelphia, 2003).

[4] M. Merz, N. Nucker, P. Schweiss, S. Schuppler, C.T. Chen, V. Chakarian, J. Freeland, Y.U. Idzerda, M. Klaser, G. Muller-Vogt, and Th. Wolf, *Phys. Rev. Lett.* **80**, 5192 (1998).

[5] V.I. Anisimov, F. Aryasetiawamn, and A.I. Lichtenstein, *J. Phys.: Condens. Matter* **9**, 767 (1997).

[6] S.G. Ovchinnikov, V.A. Gavrichkov, and M.M. Korshunov, *Physica B* **359**, 1168 (2005).

[7] I. Bozovic, G. Logvenov, M. A. J. Verhoeven, P. Caputo, E. Goldobin, and T. H. Geballe, *Nature* (London) **422**, 873 (2003).

[8] A.S. Alexandrov, in *Studies in High Temperature Superconductors,* ed. A.V. Narlikar (Nova Science Pub., NY 2006), v.**50**, pp. 1-69.

[9] A.S. Alexandrov and A.M. Bratkovsky, *Phys. Rev. Lett.* **84**, 2043 (2000).

[10] J.H. Kim, B.J. Feenstra, H.S. Somal, D. van der Marel, W.Y. Lee, A.M. Gerrits, and A. Wittlin, *Phys. Rev. B***49**, 13065 (1994).

[11] G. Zhao and D. E. Morris *Phys. Rev. B* **51**, 16487 (1995); G.-M. Zhao, M. B. Hunt, H. Keller, and K. A. Müller, *Nature* (London) **385**, 236 (1997); R. Khasanov, D. G. Eshchenko, H. Luetkens, E. Morenzoni, T. Prokscha, A. Suter, N. Garifianov, M. Mali, J. Roos, K. Conder, and H. Keller *Phys. Rev. Lett.* **92**, 057602 (2004).

[12] A. Lanzara, P.V. Bogdanov, X.J. Zhou, S.A. Kellar, D.L. Feng, E.D. Lu, T. Yoshida, H. Eisaki, A. Fujimori,K. Kishio, J.I. Shimoyana, T. Noda, S. Uchida, Z. Hussain and Z.X. Shen, *Nature* (London) **412**, 510 (2001); G-H. Gweon, T. Sasagawa, S.Y. Zhou, J. Craf, H. Takagi, D.-H. Lee, and A. Lanzara, *Nature* (London) **430**, 187 (2004); X. J. Zhou, J. Shi, T. Yoshida, T. Cuk, W. L. Yang, V. Brouet, J. Nakamura, N. Mannella, S. Komiya, Y. Ando, F. Zhou, W. X. Ti, J. W. Xiong, Z. X. Zhao, T. Sasagawa, T. Kakeshita, H. Eisaki, S. Uchida, A. Fujimori, Z.-Y. Zhang, E. W. Plummer, R. B. Laughlin, Z. Hussain, and Z.-X. Shen, *Phys. Rev. Lett.* **95**, 117001 (2005).

[13] D. Mihailovic, C.M. Foster, K. Voss, and A.J. Heeger, *Phys. Rev. B***42**, 7989 (1990).

[14] P. Calvani, M. Capizzi, S. Lupi, P. Maselli, A. Paolone, P. Roy, S.W. Cheong, W. Sadowski, and E. Walker, *Solid State Commun.* **91**, 113 (1994).

[15] R. Zamboni, G. Ruani, A.J. Pal, and C. Taliani, *Solid St. Commun.* **70**, 813 (1989).

[16] T. Timusk, C.C. Homes, and W. Reichardt, in *Anharmonic properties of High Tc cuprates* (eds. D. Mihailovic, G. Ruani, E. Kaldis, and K.A. Müller, Singapore: World Scientific, p.171

(1995)).

[17] T.R. Sendyka, W. Dmowski, and T. Egami, *Phys. Rev. B***51**, 6747 (1995); T. Egami, *J. Low Temp. Phys.* **105**, 791 (1996).

[18] A.S. Alexandrov and J. Ranninger, *Phys. Rev. B***23** 1796 (1981), ibid **24**, 1164 (1981).

[19] A.S. Alexandrov, *Russ. J. Phys. Chem.* **57** 167 (1983).

[20] J.G. Bednorz and K.A. Müller, *Z. Phys. B***64**, 189 (1986).

[21] M.K. Wu, J.R. Ashburn, C.J. Torng, P.H. Hor, R.L. Meng, L. Gao, Z.J. Huang, Y.Q. Wang, and C.W. Chu, *Phys. Rev. Lett.* **58** , 908 (1987).

[22] A.S. Alexandrov, *J. Low Temp. Phys.* **87**, 721 (1992).

[23] D. Mihailovic, V.V. Kabanov, K. Zagar, and J. Demsar, *Phys. Rev. B***60**, 6995 (1999) and references therein.

[24] A.S. Alexandrov, V.V. Kabanov, and N.F. Mott, *Phys. Rev. Lett.* **77**, 4796 (1996).

[25] A.S. Alexandrov, *Phys. Rev. B***53**, 2863 (1996).

[26] A.S. Alexandrov and P.E. Kornilovitch, *J. Phys. Cond. Matt.* **14**, 5337(2002).

[27] M. Zoli, Phys. Rev. B **57**, 555 (1998); ibid **61**, 14523 (2000).

[28] J. Bardeen, L.N. Cooper, and J.R. Schrieffer, Phys. Rev **108**, 1175 (1957).

[29] G.M. Eliashberg, *Zh. Eksp. Teor. Fiz.* **38**, 966 (1960); **39**, 1437 (1960) [*Sov. Phys. JETP* **11**, 696; **12**, 1000 (1960)].

[30] A.B. Migdal, *Zh. Eksp. Teor. Fiz.* **34**, 1438 (1958)[*Sov. Phys. JETP* **7**, 996 (1958)].

[31] A.S. Alexandrov, *Europhys. Lett.* **56**, 92 (2001).

[32] A.S. Alexandrov and P.E. Kornilovitch, *Phys. Rev. Lett.* **82**, 807 (1999); P.E. Spencer, J.H. Samson, P.E. Kornilovitch, and A.S. Alexandrov, *Phys. Rev. B***71**, 184319 (2005); J.P. Hague, P.E. Kornilovitch, A.S. Alexandrov, and J.H. Samson, *Phys. Rev. B* 73, 054303 (2006).

[33] J.P. Hague, P.E. Kornilovitch, J.H. Samson, and A.S. Alexandrov, cond-mat/0606036.

[34] H. Fehske, J. Loos, and G. Wellein, *Phys. Rev. B* **61**, 8016 (2000).

[35] J. Bonča and S. A. Trugman, *Phys. Rev. B* **64**, 094507 (2001).

[36] I.G. Lang and Yu. A. Firsov, Sov. *Phys. JETP* **16**, 1301 (1962).

[37] A.S. Alexandrov and V.V. Kabanov, *JETP Lett.*, **72**, 569 (2000).

[38] T. Mertelj, V. V. Kabanov, and D. Mihailovic, *Phys. Rev. Lett.* **94**, 147003 (2005).

[39] P.E. Kornilovitch, Phys. Rev. Lett. 81, 5382 (1998); *Phys. Rev. B* **60**, 3237 (1999).

[40] G. Verbist, F.M. Peeters, and J.T. Devreese, *Phys. Rev. B* **43**, 2712 (1991).

[41] A.S. Alexandrov, *Phys. Rev. Lett.* **82**, 2620 (1999); A.S. Alexandrov and V.V. Kabanov, *Phys. Rev. B* **59** 13628 (1999).

[42] A.S. Alexandrov, Doctoral Thesis MEPHI (Moscow, 1984); *Phys. Rev. B* **48**, 10571 (1993).

[43] A.S. Alexandrov, W.H. Beere, V.V. Kabanov, and W.Y. Liang, *Phys. Rev. Lett.* **79**, 1551 (1997).

[44] A.S. Alexandrov, *Phys. Rev. Lett.* **96**, 147003 (2006).

[45] K.K. Lee, A.S. Alexandrov, and W.Y. Liang, *Phys. Rev. Lett.* **90**, 217001 (2003); Eur. Phys. J. B **30**, 459 (2004).

[46] A.S. Alexandrov, *Phys. Rev. B* **73**(10), 100501 (2006).

[47] A.S. Alexandrov and V.N. Zavaritsky, *Phys. Rev. Lett.* **93**, 217002 (2004).

[48] A.S. Alexandrov, *Phys. Rev. Lett.* **95**, 259704 (2005).

[49] A.S. Alexandrov, cond-mat/0607770.

[50] A.S. Alexandrov and N.F. Mott, *J. Supercond* (US), **7**, 599 (1994).

[51] Z.A. Xu, N.P. Ong, Y. Wang, T. Kakeshita, and S. Uchida, *Nature* (London) **406**, 486 (2000); N.P. Ong and Y. Wang, *Physica C* **408**, 11 (2004) and references therein.

[52] V.N. Zavaritsky and A.S. Alexandrov, *Phys. Rev. B* **71**, 012502 (2005).

[53] V.N. Zavaritsky, J. Vanacken, V.V. Moshchalkov, and A.S. Alexandrov, *Eur. Phys. J. B* **42**, 367 (2004).

[54] B. Bucher, J. Karpinski, E. Kaldis, and P. Wachter, *Physica C* **167** 324 (1990).

[55] A.P. Mackenzie, S.R. Julian, G.G. Lonzarich, A. Carrington, S.D. Hughes, R.S. Liu, and D.C. Sinclair, *Phys. Rev. Lett.* **71**, 1238 (1993)

[56] M.A. Osofsky, R.J. Soulen, A.A. Wolf, J.M. Broto, H. Rakoto, J.C. Ousset, G. Coffe, S. Askenazy, P. Pari, I. Bozovic, J.N. Eckstein, and G.F. Virshup, *Phys. Rev. Lett.* **71**, 2315 (1993).; ibid **72**, 3292 (1994).

[57] D.D. Lawrie, J.P. Franck, J.R. Beamish, E.B. Molz, W.M. Chen, and M.J. Graf, *J. Low Temp. Phys.* **107**, 491 (1997).

[58] V.F. Gantmakher, G.E. Tsydynzhapov, L.P. Kozeeva, and A.N. Lavrov, *Zh. Eksp. Teor. Fiz.* **88** 148 (1999).

[59] A.S. Alexandrov, V.N. Zavaritsky, W.Y. Liang, and P.L. Nevsky, *Phys. Rev. Lett.* **76** 983 (1996).

[60] J. Hofer, J. Karpinski, M. Willemin, G.I. Meijer, E.M. Kopnin, R. Molinski, H. Schwer, C.

Rossel, and H. Keller, *Physica C* **297**, 103 (1998).

[61] V.N. Zverev and D.V. Shovkun, *JETP Lett.* **72**, 73 (2000).

[62] V.J. Emery and S.A. Kivelson, *Nature* (London), **374**, 434 (1995).

[63] A.J. Leggett, *Physica Fennica* **8**, 125 (1973); *J Stat. Phys.* **93**, 927 (1998); V.N. Popov *Functional Integrals and Collective Excitations* (Cambridge University Press, Cambridge (1987)).

[64] C. Capan, K. Behnia, J. Hinderer, A.G.M. Jansen, W. Lang, C. Marcenat, C. Martin, and J. Flouquet, *Phys. Rev. Lett.* **88**, 056601 (2002).

[65] C. Capan and K. Behnia, *Phys. Rev. Lett.* **95**, 259703 (2005).

[66] Y. Wang, L. Li, M.J. Naughton, G.D. Gu, S. Uchida, and N.P. Ong, *Phys. Rev. Lett.* **95**, 247002 (2005); L. Li, Y. Wang, M. J. Naughton, S. Ono, Y. Ando, and N.P. Ong, *Europhys. Lett.* **72**, 451(2005); Y. Wang, L. Li, and N.P. Ong, *Phys. Rev. B* **73**, 024510 (2006).

[67] A. Ettingshausen and W. Nernst, *Wied. Ann.* **29**,343 (1886).

[68] S.R. Elliot, *Physics of amorphous materials*, pp. 222-225 (Longman, New York, 1983).

[69] N.F. Mott, E.A. Davis, and R.A. Street, *Phil Mag.* **32**, 961 (1975).

[70] E.H. Sondheimer, *Proc. Roy. Soc.* **193**, 484 (1948).

[71] L. Friedman, *J. Non-Cryst.Sol.* **6**, 329 (1971); T. Holstein, *Phil Mag.* **27**, 225 (1973); D. Emin, *Phil Mag.* **35**, 1189 (1977).

[72] A.S. Alexandrov and R.T. Giles, *J. Phys.: Cond. Matt.* **9**, 9921 (1997).

[73] M. Cutler and N.F. Mott, *Phys. Rev.* **181**, 1336 (1969).

[74] A.S. Alexandrov, *Phys. Lett. A***236**, 132 (1997).

[75] C.Y. Chen, E.C. Branlund, C.S. Bae, K. Yang, M.A. Kastner, A. Cassanho, and R.J. Birgeneau, *Phys. Rev. B***51**, 3671 (1995).

[76] C. Erginsoy, *Phys. Rev.* **79**, 1013 (1950).

[77] Y. Zhang, N.P. Ong, Z.A. Xu, K. Krishana, R. Gagnon and L. Taillefer, *Phys. Rev. Lett.* **84**, 2219 (2000), and unpublished.

[78] A.S. Alexandrov and N.F. Mott, *Phys. Rev. Lett.* **71**, 1075 (1993).

[79] M. Matusiak and Th. Wolf, Phys. Rev. B**72**, 054508(R) (2005); M. Matusiak, K. Rogacki, T. Plackowski, and B. Veal, cond-mat/0412175 (2004).

[80] M.R. Li, Phys. Rev. B**65**, 184515 (2002).

[81] A. Anselm, *Introduction of Semiconductor Theory* (Prentice and Hall, New Jersey, 1981).

[82] A.S. Alexandrov, A.M. Bratkovsky, and N.F. Mott, *Phys. Rev. Lett.* **72**, 1734 (1994).

[83] W.M. Chen, J.P. Franck, and J. Jung, *Physica C* **341**, 1875 (2000).

[84] X.H. Chen, M. Yu, K.Q. Ruan, S.Y. Li, Z. Gui, G.C. Zhang, and L.Z. Cao, *Phys. Rev. B* **58**, 14219 (1998).

[85] A.S. Alexandrov, V.N. Zavaritsky, and S. Dzhumanov, *Phys. Rev. B* **69**, 052505 (2004).

[86] C. Bergemann, A.W. Tyler, A.P. Mackenzie, J. R. Cooper, S.R. Julian, and D.E. Farrel, *Phys. Rev. B* **57**, 14387 (1998).

[87] A. Junod, J-Y. Genouda, G. Trisconea, and T. Schneider, *Physica C* **294**, 115 (1998).

[88] J. Hofer, T. Schneider, J.M. Singer, M. Willemin, H. Keller, T. Sasagawa, K. Kishio, K. Conder, and J. Karpinski, *Phys. Rev. B* **62**, 631 (2000).

[89] M. J. Naughton, *Phys. Rev. B* **61**, 1605 (2000).

[90] I. Iguchi, A. Sugimoto, and H. Sato, *J. Low Temp. Phys.* **131**, 451 (2003).

[91] J.L. Tallon, J.W. Loram, J.R. Cooper, C. Panagopoulos, and C. Bernhard, *Phys. Rev. B* **68**, 180501(R) (2003).

[92] C.J. Dent, A.S. Alexandrov, and V.V. Kabanov, *Physica C* **341-348**, 153 (2000).

[93] M.R. Schafroth, *Phys. Rev.* **100**, 463 (1955).

[94] I. Bozovic, G. Logvenov, M. A. J. Verhoeven, P. Caputo, E. Goldobin, and M. R. Beasley, *Phys. Rev. Lett.* **93**, 157002 (2004).

[95] R.A. Ogg Jr., Phys. Rev. **69**, 243 (1946).

[96] M.R. Schafroth, *Phys. Rev.* **100**, 463 (1955); J.M. Blatt and S.T. Butler, *Phys. Rev.* **100**, 476 (1955).

[97] A.S. Alexandrov and V.V. Kabanov, *Sov. Phys. Solid State* **28**, 631 (1986).

[98] E.V.L. de Mello and J. Ranninger, *Phys. Rev. B* **58**, 9098 (1998).

[99] P.W. Anderson, *The Theory of Superconductivity in the Cuprates*, Princeton University Press, Princeton NY (1997).